Journal of Fluorescence (2019) 29:887–897
https://doi.org/10.1007/s10895-019-02400-5

ORIGINAL ARTICLE

Carbon Dots Green Synthesis for Ultra-Trace Determination of Ceftriaxone Using Response Surface Methodology

Narges Pourmahdi[1] · Amir H. M. Sarrafi[1] · A. Larki[2]

Received: 3 April 2019 / Accepted: 28 May 2019 / Published online: 25 June 2019

Abstract
The present study sought to develop a facile and green synthetic approach for producing fluorescent carbon dots (CDs) from a natural biomass using aqueous extraction of carbonized blue crab shell. Spherical carbon dots (6.00 ± 3.0 nm) exhibited an extended emission range with excellent quantum yield (14.5 ± 3.5%). In order to measure ceftriaxone, we offered a simple and sensitive method, based on fluorescence quenching of carbon dots in plasma and water with recovery values of 94.5–104.1%. Furthermore, with usage of central composite design (CCD) based response surface methodology (RSM); we optimized the effect of different factors. In addition, ANOVA evaluated the accuracy and suitability of quadratic model. Under optimal conditions, fluorescence quenching revealed a sensitive response in the concentration range of 20–1000 nM with the limit of detection 9.0 nM for ceftriaxone. Finally, carbon dots-based fluorescence quenching procedure was able to quantify ceftriaxone in plasma, as well as mineral and tap water. Spiked samples achieved satisfactory efficiencies.

Keywords Carbon dots · Blue crab shell · Ceftriaxone · Fluorescent probe · Central composite design

Introduction

In the recent years, more attention has been paid to quantum dots (QDs) due to the novel luminescence characterization. However, some problems limited QDs applications including complicated synthesis approach, heavy metal toxicity, and environmental hazards [1].

Photoluminescence properties of Carbon dots (CDs)(<10 nm) are similar to QDs. Additionally, they offer advantages such as water solubility, Photostability, high chemical stability, emission wavelength adjustment, low toxicity, biological availability and synthesis facility. CDs as fluorescent probes were widely replaced semiconducting QDs or fluorescent dyes utilized to measure analyte. In order to synthesis CDs, an extended range of available natural biomass such as plants [2], vegetables [3, 4], juices [5, 6], shrimp shell [6], and fish scales were used [7].

Ceftriaxone (CFX) belonging to the cephalosporin family (with long half-life) exhibits high stability and potent antibacterial activity against gram-positive and gram-negative bacteria. In addition, it is prescribed for treating septicaemia, meningitis, bronchitis Lyme (early and recovery stage after the disease), bone, joint, soft tissue, kidney and urinary tract, respiratory system (especially pneumonia), Otolaryngology, genital tract (such as gonorrhoea), skin, wound, intra-abdominal infections (peritonitis, gastrointestinal and biliary tract), infection in patients having a poor immune system, and preventing from infection during surgery [8]. Thus, in order to support patient's health, ceftriaxone amount should be monitored in biological samples. High performance liquid chromatography (HPLC) technique commonly quantifies ceftriaxone in plasma [9, 10]. Some researchers measured ceftriaxone in drug formulations using spectrophotometry [11–14], spectrofluorimetry [15, 16], Voltammetry [17], Chemiluminescence [18] and recently QDs fluorescence quenching [19, 20].

Single variable optimization approach (SVA) is a tool for optimizing in analytical chemistry [21], without

✉ Amir H. M. Sarrafi
A_mohsensarafi@iauctb.ac.ir

[1] Research Laboratory of Analytical Chemistry, Department of Chemistry, Faculty of Science, Islamic Azad University Central Tehran Branch, Tehran, Iran

[2] Department of Marine Chemistry, Faculty of Marine Science & Marine Science Research Institute, Khorramshahr University of Marine Science and Technology, Khorramshahr, Iran

regarding the combined effects of parameters, which is regarded as the main disadvantage. Consequently, the researcher implemented multivariate statistical methods such as response surface methodology (RSM), as the most appropriate one, which is considerably utilized in analytical chemistry. The RSM, as a collection of mathematical and statistical techniques, is a useful approach to determine the effects of operational parameters in optimizing and developing process. The most common and efficient RSM [22–26] is Central composite design (CCD) method.

In the present study, the researcher offered a rapid and green method for producing CDs from heated blue crab shell. Based on CDs good photoluminescence, a facile, potent, quick and non-toxic fluorescent probe was provided. Further, the effect of pH, as well as time and temperature of incubation on the fluorescent probe were examined by CCD-based RSM. Furthermore, the stability, response to interaction, and limit of detection (LOD) were assessed. Finally, CDs based optosensor was used in order to identify and quantify ceftriaxone in plasma, as well as tap and mineral water.

Materials and Methods

Materials

Sigma–Aldrich provided Ceftriaxone and quinine sulfate. The blue crab of The Persian Gulf was purchased from supermarkets and washed with double distilled water. All chemicals and reagents were of analytical grade. Thus, there is no need to further purification. Double distilled water was utilized in all experiments.

Instruments and Software

A Perkin-Elmer LS55 spectrofluorimeter was used to determine fluorescence spectra in emitting and exciting slits (band width = 5 nm). Then, absorption spectra were obtained using a Perkin-Elmer Lambda 25 spectrophotometer. Regarding Fourier transform infrared (FT-IR) spectra, a Perkin-Elmer Spectrum 400 spectrometer was implemented. JEOL JEM-2010 instrument was applied to record transmission electron microscopy (TEM) images. The X-ray photoelectron spectroscopy (XPS) analysis was conducted by VG-Microtech Multilab 3000.

To investigate the interaction between CFX and CDs, Heidolph 1000 incubator, Sonorex RK100 (Ultra Center Europe) ultrasonic bath, and Hettich D-78532 centrifuge was used. Designing an experiment, modeling surface response, and calculating optimal condition function was performed using Design Expert 10.0.1.0 software.

Synthesis of CDs

The CDs were produced via method [6] with little modification for the similarity between the raw material of the crab and shrimp (chitosan) shell. First, 5 g of blue crab shell was heated in an oven at 210 °C for 20 min. To prepare a homogeneous solution, 0.1 g of carbonized resultant was mixed with double-distilled water (1 ml) in a micro-tube and placed in an ultrasonic bath for 6 min to speed up particle scattering and CDs extracting. Finally, the solution was centrifuged at 9000 rpm for 7 min, and the supernatant solution was filtered through a cellulose acetate syringe filter (0.45 μm) and stored for further steps.

Quantum Yield of Prepared CDs

Based on the previous approach [22, 23], the quantum yield (QY) of the obtained CDs was calculated by quinine sulfate in 0.1 M H_2SO_4 ($\eta_R = 1.33$, $QY_R = 0.54$ in 360 nm) as the standard sample. The quantum yield was determined via the following equation:

$$QY_S = QY_R\left(\frac{I_S}{I_R}\right)\left(\frac{A_R}{A_S}\right)\left(\frac{\eta_S^2}{\eta_R^2}\right) \quad (1)$$

where *"I"* represents the measured integrated emission intensity, "*A*" corresponds to the absorbance on the excitation wavelength, and "η" shows the refractive index. The subscript "*S*" and "*R*" are regarded as the sample and standard.

Assay Procedure

Briefly, 200 μL of CDs homogenous solution, 400 μL Britton-Robinson buffer (pH = 5) and various amount of ceftriaxone standard solution (1 mM) was mixed. Then, double distilled water was added to attain a final volume of 5 ml. In addition, the mixture was incubated at 50 °C for 27 min. Based on fluorescence spectra of the sample and standard between 360 to 700 nm ($\lambda_{ex} = 340$ nm), the difference of the fluorescence intensity in the sample (F) versus standard (F_0) resulted in achieving responses. All the experiments were repeated 3 times.

Design of the Experiment

In this work, the effect of three variables including incubation time (10–40 min) and temperature (25-65 °C), along with pH (3–11) on the response (F_0-F), was evaluated. The optimization conditions, main parameters, and their interaction were simultaneously examined using CCD. The relevant ranges for selected variables

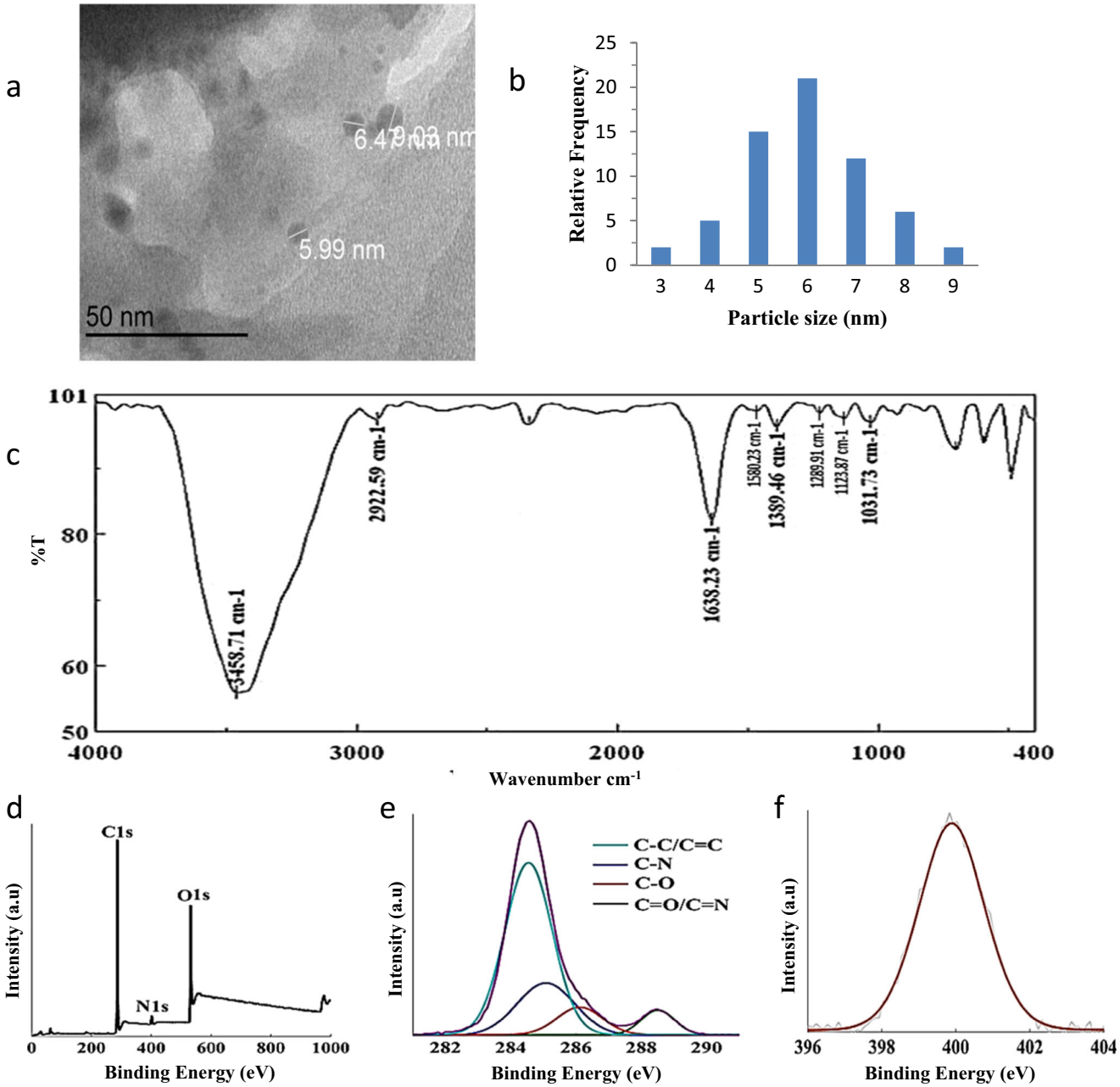

Fig. 1 **a** TEM image, (**b**) Size distribution, (**c**) FTIR spectrum, (**d**) XPS, (**e**) C1s and (**f**) N1 s XPS spectra of synthetized CDs

were chosen based on early screening study in the literature review. The factors were designed in a five-level and 20 experimental runs including six axial runs, eight cubic runs corresponding with8 runs in the full factorial, and 6 repeated runs for a central point ($\alpha = 2$). The following second-order polynomial model approximated the relationship between these independent variables:

$$Y = \beta_0 + \sum_{i=1}^{K} \beta_i X_i + \sum_{i=1}^{k} \sum_{j=i+1}^{K} \beta_{ij} X_i X_j + \sum_{i=1}^{K} \beta_{ii} X_i^2 \quad (2)$$

where X_i and X_j are considered as the main variables, β_0 represents the constant of the model, and β_i shows the linear coefficient. The coefficients of the interactive and non-linear (quadratic) effect of the main factors are β_{ij} and β_{ii}, respectively. The statistical significance of parameters, their interactions, and sufficiency of the developed regression model was assessed by ANOVA.

Sample Preparation

The ceftriaxone stock solution (1 mM) was produced with double-distilled water and stored in darkness at 4 °C prior to using. Britton-Robinson buffers were created by mixing the amounts of boric, acetic, and phosphoric acids and NaOH.

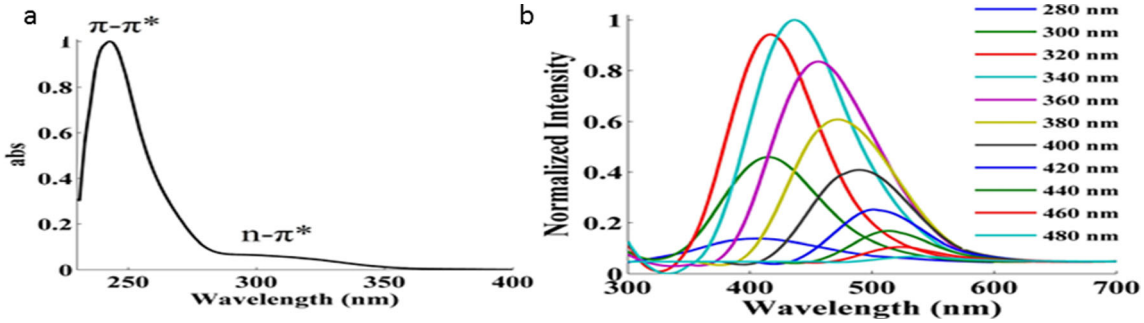

Fig. 2 **a** UV–Vis absorption, (**b**) fluorescence excitation and emission spectra of obtained CDs

The Damavand Co. and tap water samples were filtered (pore size = 0.45 μm) and directly used without early preparation. Human plasma samples were provided by the Iranian blood transfusion organization. To eliminate proteins, 1 ml of plasma was added to 1 ml of acetonitrile and centrifuged at 8000 rpm for 30 min. Subsequently, the supernatant layer was collected, and resultant acetonitrile was evaporated by passing the N_2 stream, afterward stored at 4 °C for further analysis.

Results and Discussion

Characterization of CDs

As TEM images illustrated in Fig. 1a, the CDs were dispersed appropriately and distributed in the range of 3.0–9.0 nm (Fig. 1b). In order to identify the surface functional groups in the obtained CDs, the FT-IR spectra (Fig. 1c) were utilized. The absorption bands at 3458 and 2922 cm^{-1} have corresponded to

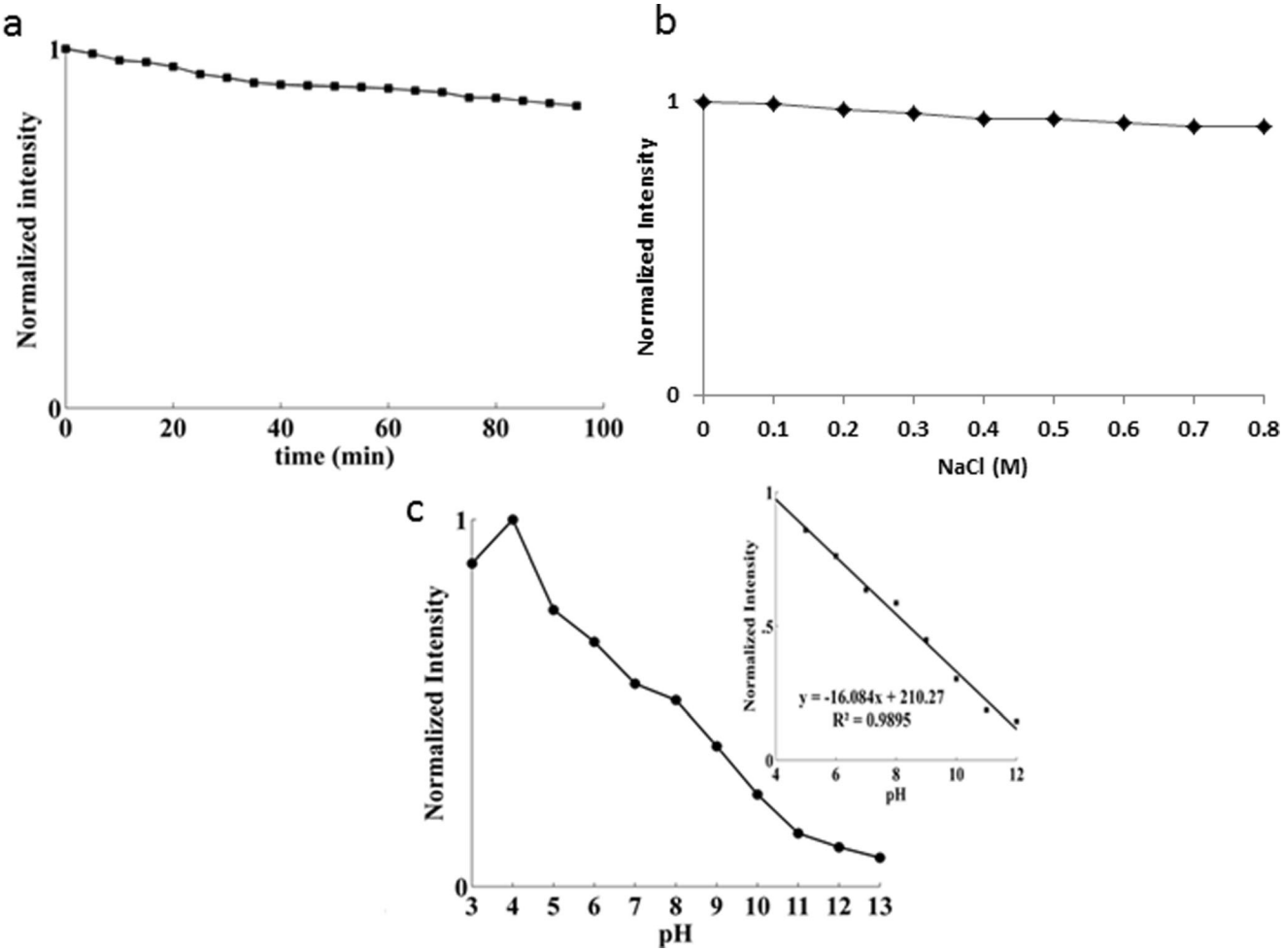

Fig. 3 **a** Stability of CDs fluorescence intensity under UV radiation, (**b**) Ionic strength effect of NaCl solution, (c) pH effect on CDs fluorescence intensity (inset: pH Linear relationship in 4–12 range)

Table 1 ANOVA for response surface quadratic model

Source	Sum of Squares	Df	Mean Square	F Value	*p* value Prob > F	
Model	43,431.96	9	4825.77	108.60	< 0.0001	significant
A-Time	482.55	1	482.55	10.86	0.0081	
B-Temp.	2915.93	1	2915.93	65.62	< 0.0001	
C-Ph	13,635.28	1	13,635.28	306.84	< 0.0001	
AB	2375.33	1	2375.33	53.45	< 0.0001	
AC	2954.90	1	2954.90	66.50	< 0.0001	
BC	789.97	1	789.97	17.78	0.0018	
A^2	16,975.32	1	16,975.32	382.01	< 0.0001	
B^2	4154.25	1	4154.25	93.49	< 0.0001	
C^2	5824.00	1	5824.00	131.06	< 0.0001	
Residual	444.37	10	44.44			
Lack of Fit	239.15	5	47.83	1.17	0.4354	not significant
Pure Error	205.22	5	41.04			
R-Squared	0.9899					
Adj R-Squared	0.9808					

C=O and C=C stretching vibrations. The stretching vibrations of tertiary C-N, C=N, C-O, and C-N were appeared in 1398, 1289, 1123 and 1031 cm^{-1}, respectively. Chemical status of CDs was characterized by XPS. Figure 1d demonstrates three signals in 285, 399.5 and 532 eV belonging to C_{1s}, N_{1s}, and O_{1s}, respectively. Based on XPS spectra of CDs, it consists of carbon, nitrogen and oxygen, as well as N- and O- doped carbon frame without any impurities (Fig. 1d). In order to sense elemental form better, C_{1s} and N_{1s} spectra were deconvoluted and fitted. C_{1s} spectrum (286.5 eV) related to C groups in C-N, C-O, C=N, C=O, C-C and C=C bonds, as well as N_{1s} peak (400.04 eV) corresponding to the fitted -NH2, indicated the existence of nitrogen and oxygen within a carbon frame of CDs (Fig. 1e, f). The presence of various oxygen and nitrogen groups on CDs resulted in improving the hydrophilic properties of CDs and acting as chromophores and auxochrome which stabilizes surface active sites, thus enhancing fluorescence activity of CDs.

Optical Properties of CDs

The optical properties of the synthesized CDs were assessed by using UV-Vis and fluorescence techniques. According to the UV-Vis spectrum (Fig. 2a), the π-π* transition of C=C and n-π* transition of C=O were exhibited two absorption peaks at 240 and 340 nm, respectively. The maximum emission of CDs centered at 412 nm with 340 nm excitation. As displayed in Fig. 2b, the emission wavelength (λ_{em}) is redshifted when the λ_{ex} changes from 280 nm to 480 nm associated with the lowered intensities. It indicates that the prepared CDs have

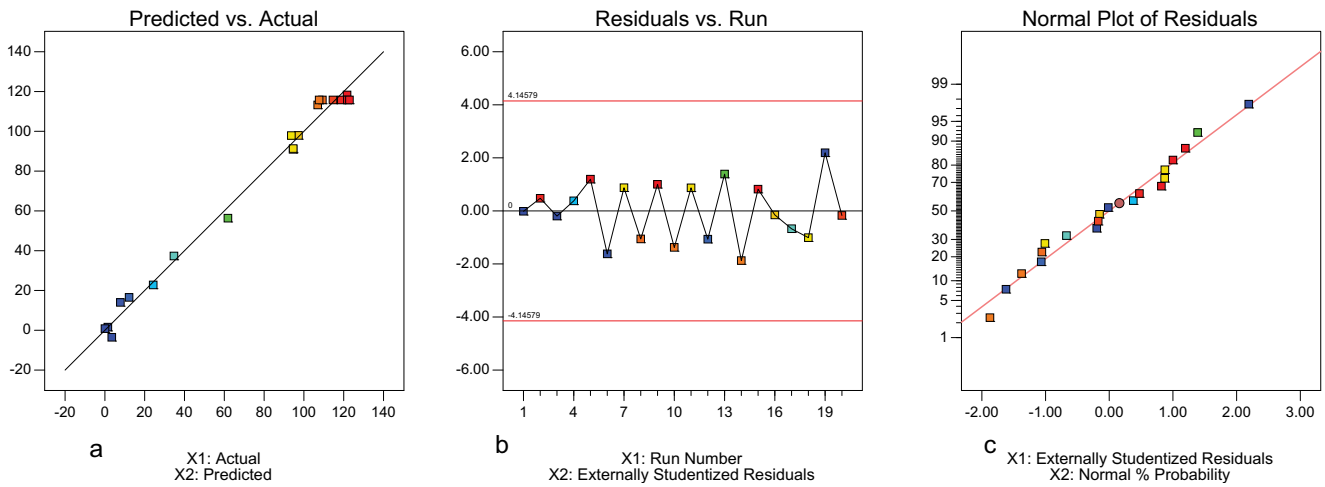

Fig. 4 **a** The predicted vs. observed response, (**b**) A plot of the externally studentized residuals vs. run number, (**c**) Normal probability plot

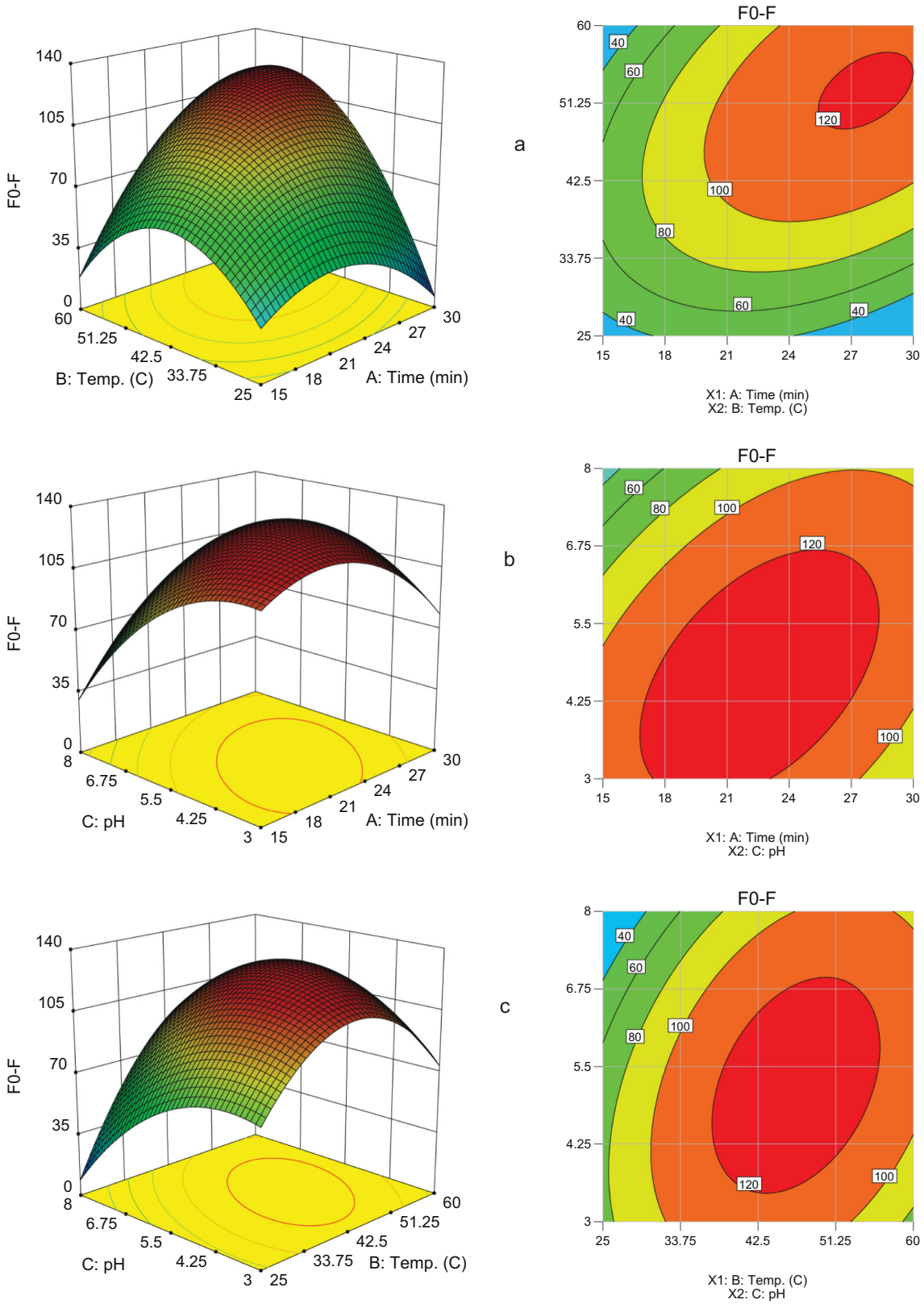

Fig. 5 3D surface response using the central composite design obtained by plotting: (**a**) Incubation time vs. temperature, (**b**) Incubation time vs. pH, (**c**) pH vs. temperature

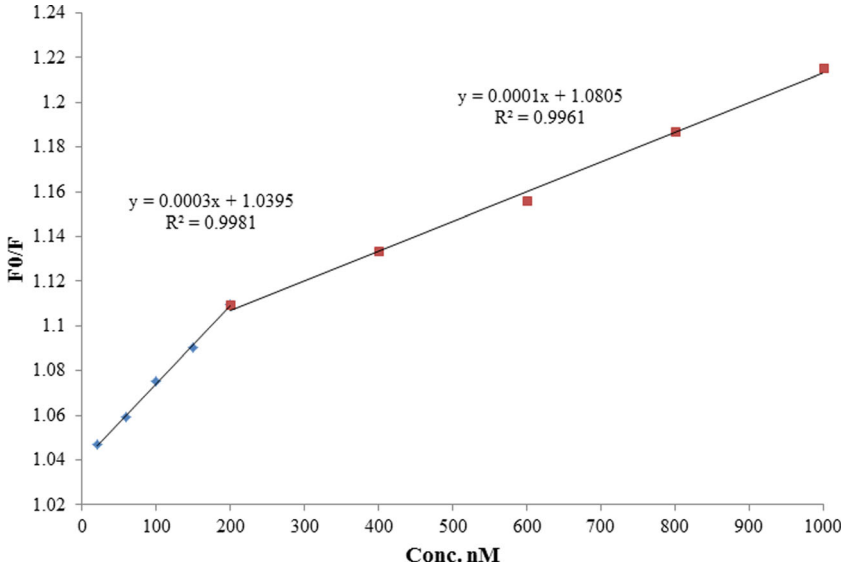

Fig. 6 Plot of (F_0/F) vs. CFX added (20–1000 nM)

λ_{ex}-dependent emission behavior, which has commonly observed in the other previous reported CDs. This behavior may be due to the different distribution of emissive energy trap, different size distribution of CDs and different surface states on CDs [27, 28].

The stability of the CDs affects their use. Its photostability was measured under UV irradiation for 100 min. The fluorescence signal reduced only 10% during the studied time, by offering good photostability (Fig. 3a). Investigating the ionic strength effect on the fluorescence intensity revealed that changing the NaCl concentration (0.1 to 0.8 M) plays a trace role on the fluorescence signal (Fig. 3b). The fluorescence intensity was estimated under a pH range of 3–13 (λ_{ex} = 340 nm), as displayed in Fig. 3c. In addition, it decreased by improving pH, and good linear behavior was observed in the pH range (4–12). The fluorescence quantum yield of the synthesized CDs was 14.5 ± 3.5%, using a reference standard of quinine sulfate.

Optimization of Sensing Conditions

Based on CCD experiments, the effects of sensing parameters, incubating time as well as temperature and varying pH (3–11) was assessed. According to the experimental data, the quadratic polynomial model was utilized for describing the response (F_0-F) and interaction between variables (eq. 3).

$$F_0-F = 42.62 + 4.52\,x_1 + 3.70\,x_2 - 15.72\,x_3 + 0.230\,x_1x_2 + 1.281x_1x_3 + 0.45\,x_2x_3 - 0.462\,{x_1}^2 - 0.129\,{x^2}_2 - 3.805\,{x_3}^2 \quad (3)$$

In this equation, x_1 and x_2 represent incubation time and temperature, and x_3 shows pH. ANOVA (Table 1) was used to assess the statistical significance of each parameter, their interactions, and the sufficiency of the calculated regression model. The proposed model was validated using the coefficient of determination (R^2 and adjusted-R^2). The R^2 (0.9899) and adjusted-R^2 (0.9808) showed a significant relationship between experimental values and model, by providing a high efficiency designed model for predicting response. Based on the ANOVA data, F-value (108.60) and *p* value (<0.0001) showed that the defined model is significant, while the lack of fit *P* value (0.4354) represented the inconsistency of the fitted model. Figure 4a illustrates a linear relationship between predicted responses versus observed data. The studentized residuals were plotted versus the run number (Fig. 4b). The random pattern of residuals represented the high effectiveness of the model and its independence on run arrangement. Based on the normal probability plot (Fig. 4c), the points were distributed normally.

In the next step, 3D surface and Contour plots were used to detect variables and their interaction on the response F_0 –F effects. A factor in the central level was kept constant, while two other factors were varied. The surface response sought to find the optimized factors at the maximum response (Fig. 5a-c).

Based on the results, an increase in pH reduced fluorescence intensity and F_0-F (Fig.5b, c). The surface hydroxyl and carbonyl groups were protonated at a strongly acidic pH. CFX as an acid (pK_a = 3.0, 3.2 and 4.1) [29] did not interact with CDs well because of inappropriate distribution in strong acidic conditions.

The maximum interaction between CFX and CDs was obtained at pH = 5, as expected. The results of Fig. 5a-c show that the addition of incubation time to 20–35 min initially increases the F_0-F response, however, the response decreases by more incubation time. The optimum parameters were calculated as incubation time = 27 min, incubation temperature = 50 °C and pH =5. At this condition, the maximum response was determined using the RSM model. The experiment repeated 5 times in optimum condition and the result was achieved 128.02 ± 2.05.

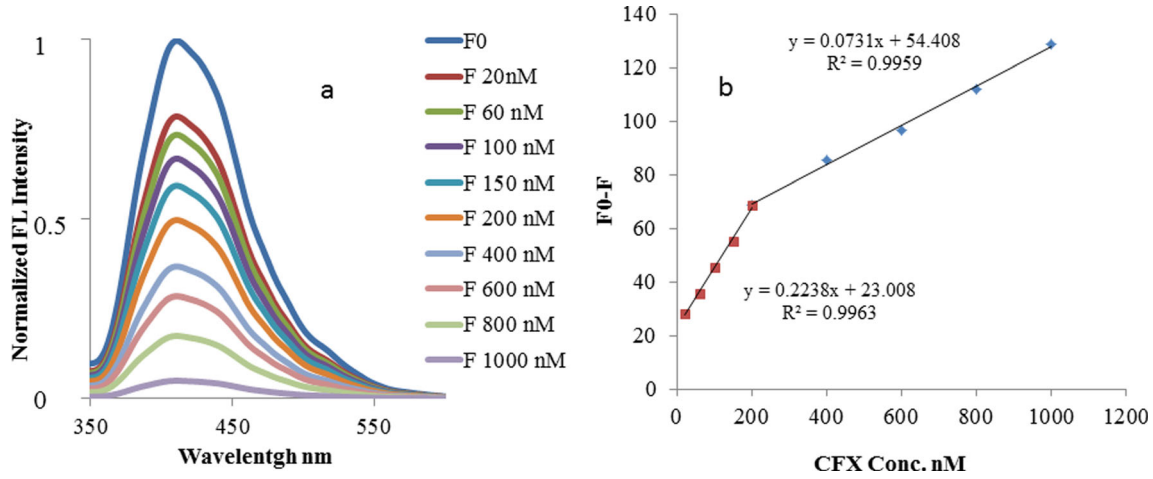

Fig. 7 **a** Fluorescence spectra of CDs before (F_0) and after CFX addition in optimum conditions, (**b**) (F0-F) vs. CFX (20–1000 nM)

Possible Fluorescence Quenching Mechanism

Quenching mechanisms of CDs include static quenching, dynamic quenching, and inner filter effect (IFE). Inner filter effect (IFE) would occur when the absorption spectrum of quencher overlapped with the excitation or emission spectra of CDs. Generally, highly effective IFE requires that the absorption band of the absorbent should overlap sufficiently with the excitation of the fluorophore and/or the emission band [30]. Ceftriaxone has a UV-Vis spectrum in 200–340 nm. The excitation wavelength used in this work was 340 nm and the emission spectrum was in 350–600 nm. The absorption spectrum of CFX did not overlap effectively with the excitation spectrum of CDs, and the absorption ability of CFX at 430 nm irradiation was very weak, suggesting that CFX could neither shield the excitation light for CDs nor absorb the emission light of CDs. Hence, the quenching mechanism in CDs-CFX system was not the inner filter effect.

Fluorescence quenching mechanism is classified to dynamic and static by colorless quenchers. Concerning static quenching mechanism, the interaction between fluorophores and quenchers resulted in forming ground state complex and failed to change chemical structure and fluorophore activity. Regarding dynamic mechanism, this interaction often results in generating ground state with weak or without fluorescence, which indicates the permeating impact between them. Fluorescence quenching behavior of CFX is analyzed by Stern-Volmer equation:

$$\frac{F_0}{F} = 1 + K_{SV}\, C_{CFX} = 1 + K_q \tau_0 C_{CFX} \qquad (4)$$

where K_{SV} represents Stern-Volmer quenching constant, K_q is the bimolecular quenching rate constant, τ_0 is the average lifetime of the molecule without quencher and C_{CFX} is regarded as the CFX concentration. Based on Eq. 4, F_0/F was plotted versus CFX concentration (Fig. 6).

For two concentration regions 20–200 and 200–1000 nM, the regression equations $F_0/F = 0.0003C_{CFX} + 1.0359$ ($R^2 = 0.9981$) and $F_0/F = 0.0001C_{CFX} + 1.0805$ ($R^2 = 0.9961$) were calculated, respectively. K_{SV}s were calculated from the slop of regression equations (3.0×10^5 $L.mol^{-1}$ and 1.0×10^5 $L.mol^{-1}$, respectively). Based on the average fluorescence

Table 2 The comparison between developed optosensor and other methods for detecting ceftriaxone

Analytical method	Linear range (μg L^{-1})	Limits of detection (μg L^{-1})	Recovery (%)	RSD (%)	References
Spectrofluoremetry	1664-55,457	555	–	<1	[19]
Voltammetry	6–5546	5	90–101	3	[17]
Chemiluminescence	11–4436	2.7	97–106	–	[18]
Spectrofluoremetry	400–20,000	1.3	97–100	5	[15]
Spectrofluoremetry	200–20,000	19.4	94–100	3	[16]
HPLC	500–250,000	170	98–102	4.67	[10]
Spectrofluoremetry MIP-GQs and MIP-CdTe QDs	0.10–50.0	0.10	83–99	<8	[20]
Spectrofluoremetry CDs	11.09–554.58	5.0	94.5–104.1	<5	The Present study

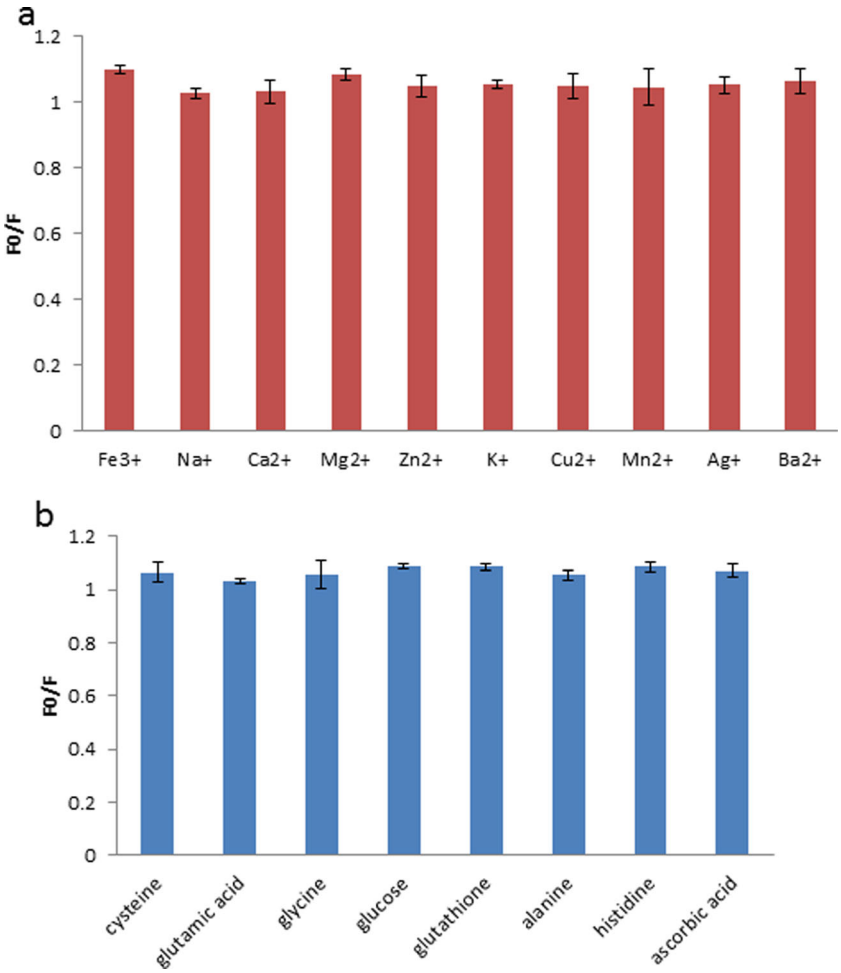

Fig. 8 Effects of (**a**) relevant metal ions, (**b**) biomolecules and other co-existing compounds on F_o-F of CDs. 200 nM CFX were used. The concentrations of interfering substances are 10 μM for K^+, Na^+, Ca^{2+}, Mg^{2+}, Zn^{2+}, Fe^{3+}, Cu^{2+}, Ag^+, Ba^{2+}, Mn^{2+}, Cysteine, Glutamic acid, glycine, glucose, glutathione, alanine, histidine and ascorbic acid. The error bars represent the standard deviation of three independent measurements

lifetime of $\tau_0 = 10^{-8}$ s [31, 32], the bimolecular quenching rate constants were calculated to be 3.0×10^{14} $Lmol^{-1}$ s^{-1} and 1.0×10^{14} $Lmol^{-1}$ s^{-1}. This value is obviously higher than the limiting diffusion constant K_{dif} of the biomolecule ($K_{dif} = 2.0 \times 10^{10}$ $Lmol^{-1}$ s^{-1}) [31, 32], which suggests that the fluorescence quenching was induced by specific interaction between CDs and CFX. These findings indicate that the quenching process may be caused by static quenching by the formation of a ground state complex. The electrostatic interactions and hydrogen bonding resulted in forming complex. XPS and FT-IR spectra confirmed the presence of -COOH, -OH and -NH2 groups on CD surface. In weak acidic pH, carboxyl and enol groups of CFX are negatively charged, while NH2 and -NH groups on CD surface are positively charged. Therefore, they are interacted electrostatically. Hydrogen bonding was simultaneously generated between oxygen atoms in CFX carbonyl group and hydrogen atoms in -NH on CD surface.

Table 3 Results of determining ceftriaxone in real sample

Sample	Spiked (nM)	Founded (nM)	Recovery% ($n = 3$)	RSD% ($n = 3$)
Plasma	0	–	–	–
	50	47.23	94.5	3.16
	100	104.13	104.1	3.48
Tap water	0	–	–	–
	50	48.50	97.0	2.64
	100	101.37	101.4	2.23
Mineral water	0	–	–	–
	50	47.28	95.6	1.80
	100	100.91	100.9	1.78

Analytical Characteristics

As shown in Fig. 7a, increasing CFX concentrations gradually reduced CD fluorescence intensities. A direct linear relationship between the response F_0–F and CFX concentrations was attained in 20–200 nM and 200–1000 nM ranges with regression equations of (F_0-F) =0.2177C_{CFX} + 23.199 (R^2 = 0.9958) and (F_0-F) = 0.074C_{CFX} + 53.695 (R^2 = 0.9957), respectively (F and F_0 illustrate the fluorescence intensities of CDs in the presence and absence of CFX, while C_{CFX} is considered as CFX concentration) (Fig. 7b). The limit of detection (LOD) for CFX was quantified at 8.9 nM (S/*N* = 3). The analytical features of the present study are consistent with the reported literature regarding CD-based CFX nano-sensors (Table 2).

Investigating Potential Interferences

To examine the analytical application of our proposed method in real samples, the effects of potential interfering substances such as metal ions (Fe^{3+}, Na^{+}, Ca^{2+}, Mg^{2+}, K^{+}, Cu^{2+}, Mn^{2+}, Ag^{+}, Ba^{2+}, Cr^{3+}), organic compounds (cysteine, glutamic acid, glycine, glucose, glutathione, alanine, histidine, ascorbic acid), which were available in water and plasma real samples were assessed. CFX could significantly affect CDs fluorescence intensity, while a slight increase in CDs fluorescence was observed for other interfered substances (Fig. 8).

Real Samples Analysis

Finally, the suggested approach was implemented for detecting CFX in some real samples such as mineral and tap water and human plasma (Table 3). Standard addition method was applied in recovery studies. The results for plasma and water (94.5–104.1 and 95.6–101.4, respectively) offered the applicability of the method for detecting CFX in real samples.

Conclusion

The present study aimed to synthesize CDs through a facile, green, rapid and cost-efficient method to develop the appropriate and sensitive optosensor for detecting trace amounts of CFX in real samples. The goat CDs were fluorescence nano-sensors for sensitive and selective detection of CFX. The experimental parameter effects on the fluorescence quenching of CFX were mathematically evaluated using CCD-based RSM. Regarding CFX, the linear response ranges were 20–200 and 200–1000 nM, while the limit of detection was obtained at 8.9 nM. This fluorescent nano-sensor was successful in detecting CFX in real samples. The proposed CDs-based nano-sensor proposed a quick and assay for detecting CFX, especially in clinical and environmental tests.

Acknowledgements The authors thank the research laboratories of chemistry in Central Tehran Branch, Islamic Azad University for their support this study.

Compliance with Ethical Standards

Conflict of Interest The author declares that there is no conflict of interest.

References

1. Lin FE, Gui C, Wen W, Bao T, Zhang X, Wang S (2016) Dopamine assay based on an aggregation-induced reversed inner filter effect of gold nanoparticles on the fluorescence of graphene quantum dots. Talanta 158:292–298. https://doi.org/10.1016/j.talanta.2016.05.062
2. Liu S, Tian JQ, Wang L, Zhang YW, Qin XY, Luo YL, Asiri AM, Al-Youbi AO, Sun XP (2012) Hydrothermal treatment of grass: a low-cost, green route to nitrogen-doped, carbon-rich, photoluminescent polymer nanodots as an effective fluorescent sensing platform for label-free detection of cu(II) ions. Adv Mater 24:2037–2041. https://doi.org/10.1002/adma.201200164
3. Niu XQ, Liu GS, Li LY, Fu Z, Xu H, Cui FL (2015) Green and economical synthesis of nitrogen-doped carbon dots from vegetables for sensing and imaging applications. RSC Adv 5:95223–95229. https://doi.org/10.1039/C5RA17439B
4. Jin H, Gui RJ, Wang YF, Sun J (2017) Carrot-derived carbon dots modified with polyethyleneimine and nile blue for ratiometric two-photon fluorescence turn-on sensing of sulfide anion in biological fluids. Talanta 169:141–148. https://doi.org/10.1016/j.talanta.2017.03.083
5. Miao H, Wang L, Zhuo Y, Zhou ZN, Yang XM (2016) Label-free fluorimetric detection of CEA using carbon dots derived from tomato juice. Biosens Bioelectron 86:83–89. https://doi.org/10.1016/j.bios.2016.06.043
6. Lina P, Hsieha C, Kung M, Chua L, Huang H, Chen H, Wud D, Kuod C, Hsieh S (2014) Eco-friendly synthesis of shrimp egg-derived carbon dots for fluorescent bioimaging. J Biotechnol 189:114–119. https://doi.org/10.1016/j.jbiotec.2014.08.043
7. Zhang Y, Gao Z, Zhang W, Wang W, Chang J, Kai J (2018) Fluorescent carbon dots as nanoprobe for determination of lidocaine hydrochloride. SENSOR ACTUAT B-CHEM 262:928–937. https://doi.org/10.1021/ja062677d
8. da Trindade MT, Salgado HRN (2018) A critical review of analytical methods for determination of ceftriaxone sodium. Crit Rev Anal Chem 48(2):95–101. https://doi.org/10.1080/10408347.2017.1398063
9. Brayfield A, Martindale A (2014) The complete drug reference. Pharmaceutical Press, London
10. Shah J, Jan MR, Shah S, Khan MN (2013) Development and validation of HPLC method for simultaneous determination of ceftriaxone and Cefaclor in commercial formulations and biological samples. *J* Mex *Chem Soc* 57:314–320. https://doi.org/10.1155/2014/278173
11. Rageh AH, El-Shaboury SR, Saleh GA, Mohamed FA (2010) Spectophotometric method for determination of certain Cephalosporins using 4-Chloro-7-Nitrobenzo-2-Oxa-1, 3-diazole (NBD-cl). Nat Sci 8:828–840. https://doi.org/10.4236/ns.2010.28104
12. Pasha C, Narayana B (2008) A simple method for the spectrophotometric determination of Cephalosporins in pharmaceuticals using Variamine blue. Eclet Quím 33:41–46. https://doi.org/10.1590/S0100-46702008000200006

13. Saleh GA, Askal HF, Darwish IA, El-Shorbagi AA (2003) Spectroscopic analytical study for the charge-transfer complexation of certain Cephalosporins with Chloranilic acid. Anal Sci 19:281–287. https://doi.org/10.2116/analsci.19.281
14. Ethiraj R, Thiruvengadam E, Sampath, VS, Vahig A, Raj J (2014) Development and Validation of Stability Indicating Spectroscopic Method for Content Analysis of Ceftriaxone Sodium in Pharmaceuticals. Int Sch Res Notices. https://doi.org/10.1155/2014/278173
15. Shah J, Jan MR, Shah S (2013) Development and validation of a Spectrofluorimetric method for the quantification of ceftriaxone in pharmaceutical formulations and plasma. Luminescence 28:516–522. https://doi.org/10.1002/bio.2487
16. Shah J, Jan MR, Shah S, Naeem M (2011) Spectrofluorimetric protocol for ceftriaxone in commercial formulation and human plasma after condensation with formaldehyde and ethylacetoacetate. J Fluoresc 21:2155–2163. https://doi.org/10.1007/s10895-011-0917-0
17. Karpov VM, Spektor DV, Beklemishev MK (2016) Determination of ceftriaxone by the fluorescence quenching of quantum dots using binding with polyethyleneimine. J Anal Chem 71:519–526. https://doi.org/10.1134/S1061934816050051
18. Shahrokhian S, Hosseini-Nassab N, Kamalzadeh Z (2014) Fabrication of an electrochemical sensor based on the electrodeposition of Pt nanoparticles on multiwalled carbon nanotubes film for voltametric determination of ceftriaxone in the presence of lidocaine, assisted by factorial-based response-surface methodology. J SOLID STATE ELECTR 18:77–88. https://doi.org/10.1007/s10008-013-2243-8
19. Abolhasani J, Hassanzadeh J (2014) Potassium permanganate-acridine yellow chemiluminescence system for the determination of fluvoxamine, isoniazid and ceftriaxone. Luminescence 29:1053–1058. https://doi.org/10.1002/bio.2659
20. Chullasat K, Kanatharana P, Bunkoed O (2018) Nanocomposite optosensor of dual quantum dot fluorescence probes for simultaneous detection of cephalexin and ceftriaxone. SENSOR ACTUAT B-CHEM 281:689–697. https://doi.org/10.1016/j.snb.2018.11.003
21. Czitrom V (1999) One-factor-at-a-time versus designed experiments. Am Stat 53(2):126–131
22. Nemati F, Zare-Dorabei R, Hosseini M, Ganjali MR (2018) Fluorescence turn-on sensing of thiamine based on arginine – functionalized graphene quantum dots (Arg-GQDs): central composite design for process optimization. SENSOR ACTUAT B-CHEM 255(2):2078–2085. https://doi.org/10.1016/j.snb.2017.09.009
23. Nemati F, Hosseini M, Zare-Dorabei R, Salehnia F, Ganjali MR (2018) Fluorescent turn on sensing of caffeine in food sample based on sulfur-doped carbon quantum dots and optimization of process parameters through response surface methodology. SENSOR ACTUAT B-CHEM 273:25–34. https://doi.org/10.1016/j.snb.2018.05.163
24. Mosleh M, Ghoreishi SM, Masoum S, Khoobi A (2018) Determination of quercetin in the presence of tannic acid in soft drinks based on carbon nanotubes modified electrode using chemometric approaches. SENSOR ACTUAT B-CHEM 272:605–611. https://doi.org/10.1016/j.snb.2018.05.163
25. Baghi Sefidan S, Eskandari H, Shamkhali AN (2018) Rapid colorimetric flow injection sensing of hypochlorite by functionalized graphene quantum dots. SENSOR ACTUAT B-CHEM 275:339–349. https://doi.org/10.1016/j.snb.2018.08.023
26. Hashemi F, Rastegarzadeh S, Pourreza N (2018) Response surface methodology optimized dispersive liquid–liquid microextraction coupled with surface plasmon resonance of silver nanoparticles as colorimetric probe for determination of captopril. SENSOR ACTUAT B-CHEM 256:251–260. https://doi.org/10.1016/j.snb.2017.09.178
27. Liu L, Mi Z, Hu Q, Li C, Li X, Feng F (2018) One-step synthesis of fluorescent carbon dots for sensitive and selective detection of hyperin. Talanta 186:315–321. https://doi.org/10.1016/j.talanta.2018.04.065
28. Huang S, Wang L, Huang C, Xie J, Su W, Sheng J, Xiao Q (2015) A carbon dots based fluorescent probe for selective and sensitive detection of hemoglobin. SENSOR ACTUAT B-CHEM 221:1215–1222. https://doi.org/10.1016/j.snb.2015.07.099
29. Brittain HG (2000) Analytical profiles of drug substances, excipients, and related methodology. Elsevier Academic Press, New York
30. Chen S, Yu YL, Wang JH (2017) Inner filter effect-based fluorescent sensing systems: a review. Anal Chim Acta 999:13–26. https://doi.org/10.1016/j.aca.2017.10.026
31. Zhao C, Jiao Y, Hu F, Yang Y (2018) Green synthesis of carbon dots from pork and application as nanosensors for uric acid detection. Spectrochim Acta A Mol Biomol Spectrosc 190:360–367. https://doi.org/10.1016/j.saa.2017.09.037
32. Zhang Y, Gao Z, Zhang W, Wang W, Chang J, Kai J (2018) Fluorescent carbon dots as nanoprobe for determination of lidocaine hydrochloride. SENSOR ACTUAT B-CHEM 262:928–937. https://doi.org/10.1016/j.snb.2018.02.079